ACS OMEGA

Open Access

http://pubs.acs.org/journal/acsodf

Article

3D-Printed Smartwatch Fabricated via Vat Photopolymerization for UV and Temperature Sensing Applications

Fahad Alam, Aljawharah Alsharif, Fhad O. AlModaf, and Nazek El-Atab*

Cite This: *ACS Omega* 2024, 9, 14830−14839

Read Online

ACCESS | Metrics & More | Article Recommendations | Supporting Information

ABSTRACT: Ultraviolet (UV) exposure overdose can cause health issues such as skin burns or other skin damage. In this work, a UV and temperature sensor smartwatch is developed, utilizing a multimaterial 3D printing approach via a vat photopolymerization−digital light processing technique. Photochromic (PC) pigments with different UV sensitivities, UVA (315−400 nm) and UVB (315−280 nm), were utilized to cover a wider range of UV exposure and were mixed in transparent resin, whereas the smartwatch was printed with controlled thickness gradients. A multifunctional sensor was next fabricated by adding a thermochromic (TC) material to PC, which is capable of sensing UV and temperature change. Colorimetric measurements assisted by a smartphone-based application provided instantaneous as well as cumulative UV exposure from sunlight. The mechanical properties of the device were also measured to determine its durability. The prototype of the wearable watch was prepared by fixing the 3D-printed dial to a commercially available silicon wristband suitable for all age groups. The 3D-printed watch is water-resistant and easily removable, allowing for its utilization in multiple outdoor activities. Thus, the developed wearable UV sensor alerts the user to the extent of their UV exposure, which can help protect them against overexposure.

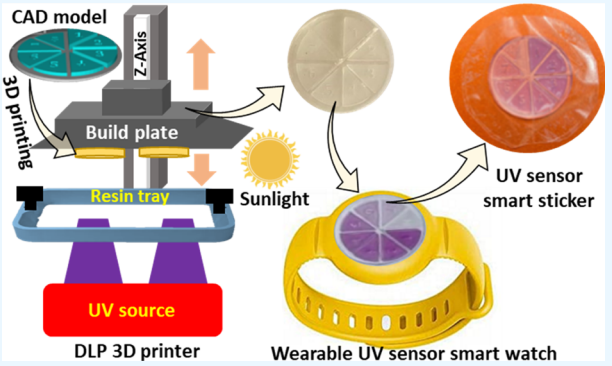

1. INTRODUCTION

Ultraviolet rays from sunlight are the main cause of skin damage, such as sunburns, premature skin aging, and sometimes cancer.[1] In general, the human body is exposed to UV radiation during daily outdoor activities such as sports, school, and outdoor work. While UV radiation is beneficial to the human body up to a certain level of exposure, beyond that limit, it becomes harmful, and an overdose of UV can cause health issues[2] such as sunburn and skin cancer.[3] Therefore, it is crucial to have the correct information about the safety limits, that is, daily limits of UV radiation dosage for precautions. Based on daily exposure and harmful effects of UV radiation, it is very important to keep track of the UV exposure.[4] The UV band includes a wavelength range between 200 and 400 nm and is categorized as UVA (315−400 nm), UVB (315−280 nm), or UVC (280−100 nm).[5] Among all of the UV ranges, UVA is the most common and harmful to human beings.[6] Unlike other adverse weather conditions, such as storms, rain, or pollution, UV radiation exposure cannot be observed by the naked eye; therefore, a sensor is required to monitor it.[7] There are various methods to protect the body from overexposure to UV radiation, including the application of sunscreens,[8] nanoparticles,[9] UV-impermeable clothes for UV weakening,[10] glasses to protect the eyes,[11] and textile to protect most of the body parts.[12] Although these methods provide sufficient protection from UV exposure, they do not give any information about the extent of UV radiation exposure or the exposure threshold to avoid UV overdose. Various tools are available for monitoring UV light; however, most are not wearable and require electronic components and power supplies for measurements.[13]

Furthermore, these tools cannot detect instantaneous and cumulative UV radiation exposure as well as temperature changes, simultaneously. The reversible color switching in the presence of radiation is called photochromism, and such materials are called photochromic (PC) materials.[14,15] The PC materials have gained huge attention because their optical properties can be changed by the application of UV radiation as an external stimulus.[16] The PC materials are classified into two categories: thermally unstable (T-type) and thermally stable (P-type) photogenerated optical isomers.[17] T-type PC materials change color under heat, whereas P-type PC materials change color under UV light. Therefore, P-type PC materials can be potentially used for sustainable applications such as display materials decorative items, optical memory devices, and PC optical sensors.[15,18] Colorimetric sensors

Received: September 25, 2023
Revised: March 7, 2024
Accepted: March 11, 2024
Published: March 20, 2024

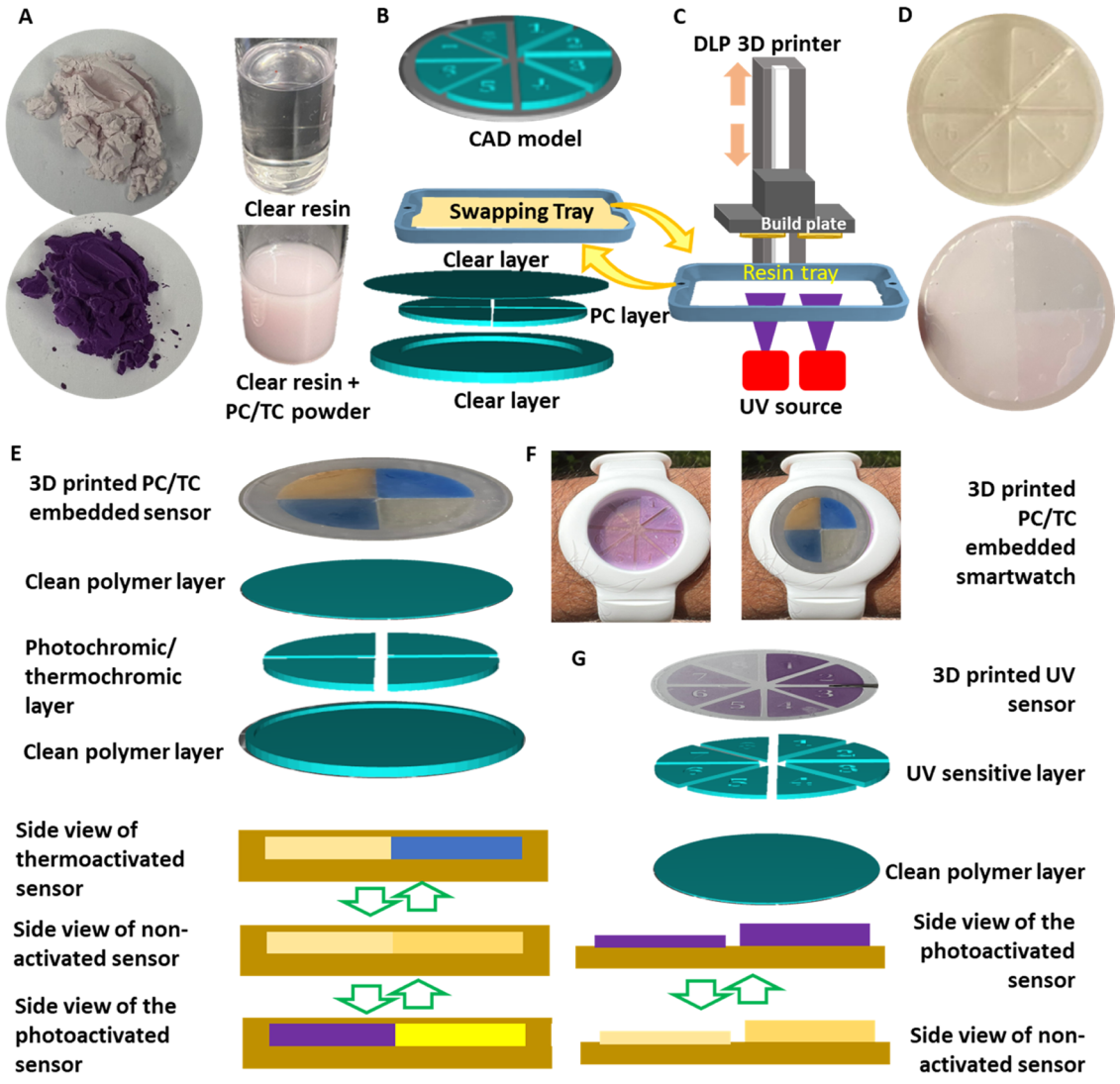

Figure 1. Process of 3D printing of smart UV sensor watch. (A) Digital photograph of one of the photochromic pigment powders used in the current study. The color switches from white to colorful upon exposure to UV light. The pigment powder is mixed with the clear resin as shown in the bottom. (B) Process of 3D printing showing the CAD model and slicing the model. (C) Schematic representation of the DLP and tray swiping mechanism for obtaining the multimaterial 3D-printed specimen. (D) Digital photographs of the 3D-printed smartwatch along with the activated photographs. (E) Schematic representation and digital photographs of the 3D-printed multifunction UV-temperature sensor. (F) 3D-printed smartwatch while operating. (G) Schematic representation and digital photographs of the 3D-printed UV indicator.

based on photochromic materials[19] are alternatives to electronic UV sensors that can be used for UV exposure monitoring; however, the fabrication of complex structures with an appropriate readout is a challenge. Thermochromic materials have recently been utilized for sensing temperature changes by colorimetric measurements.[20,21] A sensor embedded with PC and thermochromic TC materials can simultaneously sense UV radiation and temperature changes.[16] Qinghua Meng et al. developed a smartphone-based sensor for UV index, but the manufacturing method utilized was coating of photochromic material.[22] To enhance the repeatability and durability of the wearable sensor, advanced technologies such as additive manufacturing can be used for their manufacture. The advent of 3D printing has enabled the fabrication of complex structures with the controlled growth of multiple materials for colorimetric sensing applications.[23] Among the various 3D printing techniques,[24] a vat-photopolymerization-based technique[25] called digital light processing (DLP) allows for the fabrication of composite materials by mixing filler particles in the resin.[20,21,26] In addition to the advantage of composite material printing, DLP allows multimaterial printing by simply swapping trays.[27,28] The 3D printing of composite materials enables sensing properties with a desktop DLP 3D printer, which in the current work is customized such that more than 2 materials can be printed using the same printer. The multimaterial 3D printing approach[27] would enable the fabrication of multifunctional colorimetric sensors.

In this study, we developed a wearable watch/patch via a vat-photopolymerization-based 3D printing method. The method was designed to achieve multimaterial printing and obtain a significant colorimetric sensor readout. The developed sensor is durable and reusable and is suitable for all age groups. The developed wearable device reports personal UVA and UVB exposure and temperature changes during real-time outdoor activities. The photosensitive pigment sensitive to various UV ranges was employed in the device, which changes color when exposed to sunlight and provides the readout for UV measurements. Moreover, TC was added to sense

https://doi.org/10.1021/acsomega.3c07411
ACS Omega 2024, 9, 14830−14839

temperature changes in the ambient environment. To quantify the readout, a smartphone-based application called ColorPicker was utilized to pick the RGB (red, green, and blue) from the captured photo. Subsequently, the RGB values were correlated with the exposure time, indicating the extent of UV exposure. The developed device is portable and can be operated without additional electrical components while measuring UV exposure.

2. EXPERIMENTAL DESIGN

2.1. Materials. A commercial transparent resin (Ultraclear 405 nm Rapid Curing Resin from NOVA3D 3D Printer) was obtained and utilized for 3D printing of the base of the UV sensor watch. Isopropyl alcohol (IPA) purchased from Merck (Darmstadt, Germany) was used to wash the 3D-printed samples. Nontoxic PC pigment powders (p-type) of three different colors (purple, blue, yellow, and orange) and a TC powder (blue), sensitive to the temperature change from 25 to 40 °C, were purchased from Atlanta Chemical Engineering LLC and used as purchased.

2.2. Methods. *2.2.1. Preparation of Thermochromic Resin.* To prepare the photochromic and thermochromic resins, the PC and TC pigment powders were mixed with the commercial transparent resin and used for 3D printing. Mixing was performed by adding the transparent resin to a beaker, and then 1 wt % of the PC pigment powders of three different colors (purple, blue, and orange) and blue-colored TC were added to the beaker under stirring condition. The PC powders were added to achieve a visible color change in response to UV rays from sunlight while TC changes its color from blue to transparent upon rise in temperature from 25 to 40 °C. The pigment-mixed resin was prepared just before 3D printing just to make sure that the pigment powders were dispersed uniformly when poured into a resin tray.

2.2.2. CAD Models Preparation. The designs for the UV sensor smartwatch and test specimens for bending and tensile tests for 3D printing were prepared via a computer-aided design tool (CAD) called SOLIDWORKS. The files were saved in the standard triangle language (.stl) format which is the required input format for most of the slicing tools, Phtoton_workshop_V2.1.29, available with 3D printers.[29] Screenshots of the CAD model are shown in Figure 1B.

2.2.3. DLP 3D Printing. A UV sensor smartwatch was fabricated by using a DLP 3D printer (Anycubic Photon S MONO). The printer illuminates a UV light of 405 nm wavelength through a 6 in. 2K Monochrome Liquid Crystal Display (LCD) screen with 2560 × 1620 pixels, XY resolution of 52 μm, and *Z*-axis resolution (layer thickness) of 10 μm. The resin was cured by DLP through its high-resolution LCD screen, which functions as a projector. The photosensitive resin was placed in a resin tray prior to printing, and UV light was illuminated from the bottom of the clear resin vats to cure each layer of the object as it adhered to the print bed. After each layer was cured, the print bed was raised according to the chosen layer thickness (50 to 100 μm) to make room for the next layer. The resin vat and build plate were protected from ambient UV light by a hood. The 3D CAD models were sliced into layers using the software Photon Workshop V2.1.29.RC12. The optimized parameters for the 3D printing process of the smartwatch are mentioned in Table 1.

2.3. Characterization. The 3D-printed sensor was analyzed for its microstructural, optical, and physical properties. The microstructures of the photochromic pigment powders and the cross sections of the 3D-printed thermochromic optical fibers were observed using scanning electron microscopy (SEM; Teneo, FEI Co.), at an operating voltage of 5 and a spot size of 2.5 mm at a working distance (WD) of 10 mm. To make the surface conductive, a thin layer (∼5 nm) of iridium was coated on the samples before SEM observation. The 3D-printed samples were fractured cryogenically, and the cross sections were observed to see the internal morphology and dispersion of pigment powders. The optical transparency was observed by using UV−vis spectroscopy, and the optical transmission of the 3D-printed sensor was observed. A UV−vis spectrophotometer (UV−vis−NIR Lambda 950) with a detection range of 200−2400 nm was used to investigate the light transmission from 3D-printed transparent and tinted with PC pigments powder samples. The results were presented in terms of % transmission intensity with respect to the wavelength (nm). For measurement temperature sensing capability of the 3D-printed multifunctional sensor, the temperature was increased in a controlled fashion utilizing a hot plate from 25 to 40 °C with an interval of 2 °C and the digital photos were captured. Both optical isomeric shapes of photochromic and thermochromic pigments will reflect light differently and generate the emission color within the RGB system. Change in color can be detected via the camera of a smartphone. The RGB values were measured with the help of the ColorPicker smartphone application and presented. Furthermore, the *g* value (G/R+G+B) was calculated from the RGB values to correlate with the UV index. The camera of a smartphone is utilized to capture photos, indoor and outdoor, and the results obtained are presented on the basis of the photos captured. Since the target is to develop a wearable device that should be robust and easy to handle, the use of the complicated photographic setup is avoided. However, to keep the uniformity in the results, all of the photographs are captured in the noon time at the same location. The mechanical properties of the 3D-printed transparent, tinted, and tinted with UV-exposed sample were characterized by tensile and three-point bending tests. ASTM D638 (type IV) standard samples were 3D-printed and tested under quasi-static uniaxial tensile test conditions using a uniaxial tensile machine. (UTM, ZwickRoell Z005, Germany) equipped with a 2.5 kN load cell.[30] The tests were conducted under controlled conditions with a constant crosshead speed of 5 mm/min at a normal room temperature of approximately 25 °C. The load−displacement curves obtained from the tensile test experiments were used to derive the stress−strain curves. The stress values were determined by using a cross-sectional area of 13 × 3 mm, and a gauge length of 50 mm was used to calculate the strain at each point. The three-point bending test was performed following the ASTM D790 standard on a flat rectangular bar (80 × 12.7 × 3 mm).[20,31] The elastic modulus, ultimate tensile strength, and elongation/deflection were calculated from the stress−strain curves and reported as the average of the three tests.

Table 1. 3D Printing Parameters Optimized for the Fabrication Process for a Smartwatch

printing parameters	specifications
layer thickness	50 μm
curing time	burn layers −15 s, normal layers −5 s
print speed	5 s per layer
support	no support, printed directly on the build plate

https://doi.org/10.1021/acsomega.3c07411
ACS Omega 2024, 9, 14830−14839

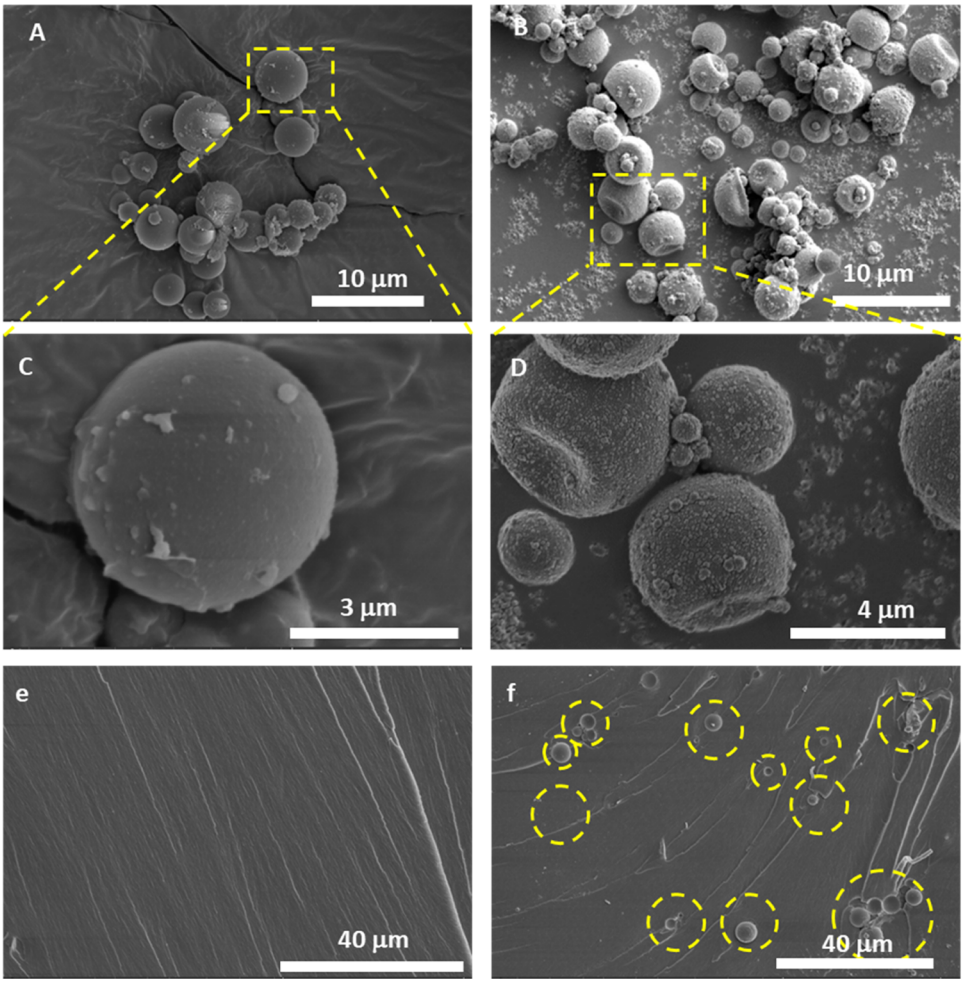

Figure 2. SEM micrographs of the PC, TC pigment powders, and the cross section of the 3D-printed samples: (A) photochromic pigment powders, (B) thermochromic pigment powder, (C) magnified position of dotted box present in (A), (D) magnified position of dotted box present in (B), (e) cross section of the 3D-printed transparent sample (resin only), and (f) cross section of the 3D-printed sample mixed with pigment powder.

The values of flexural stress (σ_f), flexural strain (ε_f), and elastic modulus during 3-point bending tests (E_B) were calculated using the below equations

$$\sigma_f = 3P_iL/2bd^2 \quad (1)$$

$$\varepsilon_f = 6Dd/L^2 \quad (2)$$

$$E_B = L^3M/4bd^2 \quad (3)$$

where P_i is the load at a specific point on the load vs displacement curve, L denotes the span between the support, b and d represent the width and depth of the specimen, respectively, and D represents the maximum deflection of the center of the specimen. The dimensions of the test specimens are shown in Figure SI1.

3. RESULTS AND DISCUSSION

The surfaces of the PC and TC pigment powders and the cross sections of the 3D-printed samples were observed under SEM, and the results are presented in Figure 2. The micrographs of the photochromic (Figure 2A) and thermochromic (Figure 2B) pigment powders confirm their spherical geometry with a size of approximately 5 μm. The 3D-printed samples from the transparent resin (clear) and resin mixed with pigment powder (tinted) were fractured cryogenically, and their cross sections were observed. The results for the clear and tinted samples are presented in Figure 2C,D, respectively. The uniformity and smoothness in the micrographs in Figure 2C indicate that no filler particles are present, whereas in Figure 2D, the presence of uniformly distributed spherical particles confirms the even distribution of the pigment powders.

The smartwatch embedded with photochromic pigments was printed with four and eight compartments with a thickness gradient to obtain the UV sensing response. The CAD models were designed with numbers embedded in each compartment. The lower the number written in the compartment, the greater the thickness. Consequently, the greater the thickness, the greater the photochromic pigment content. Because the thicker compartments contain a higher amount of PC pigment, their color changes faster when exposed to UV light. The compartment with the lowest thickness was the last to change color, indicating a longer UV light exposure. As highlighted in Figure 3A,B, the color change starts from the thicker portion and progresses gradually to the thinner portion. This gradual change in color according to the thickness correlates with the UV exposure time. To estimate UV exposure, the color of the activated portion was observed using a smartphone application that provides the RGB segment of the color. The RGB values

https://doi.org/10.1021/acsomega.3c07411
ACS Omega 2024, 9, 14830−14839

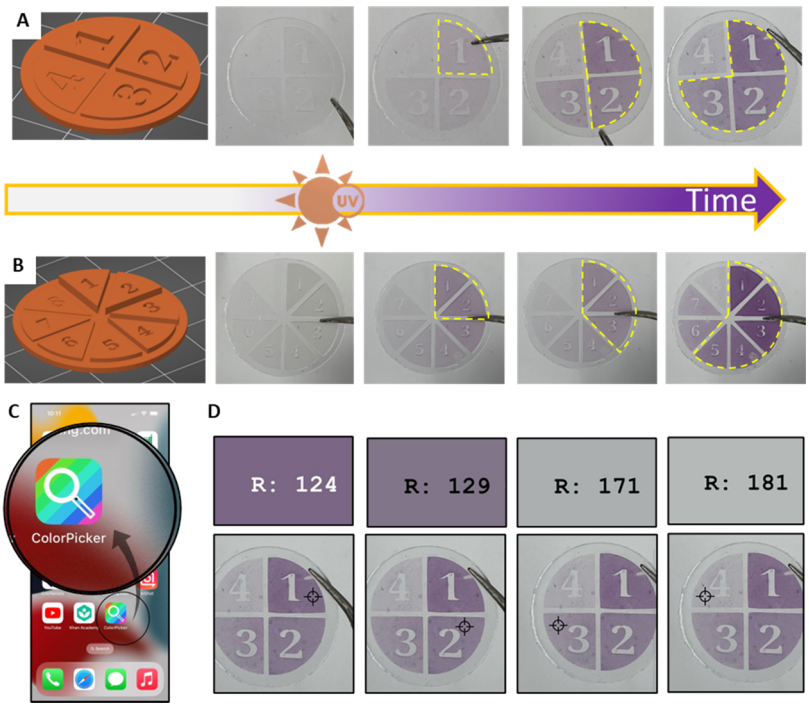

Figure 3. UV indication with the help of a 3D-printed sensor. (A, B) Gradient UV sensitivity with a level 4-grade UV exposure. (C) The smartphone application ColorPicker was used to determine the RGB components from each photograph taken at different UV exposure times. (D) The *R* values detected by the mobile application were taken from the different spots on the watch as indicated by the circular dots.

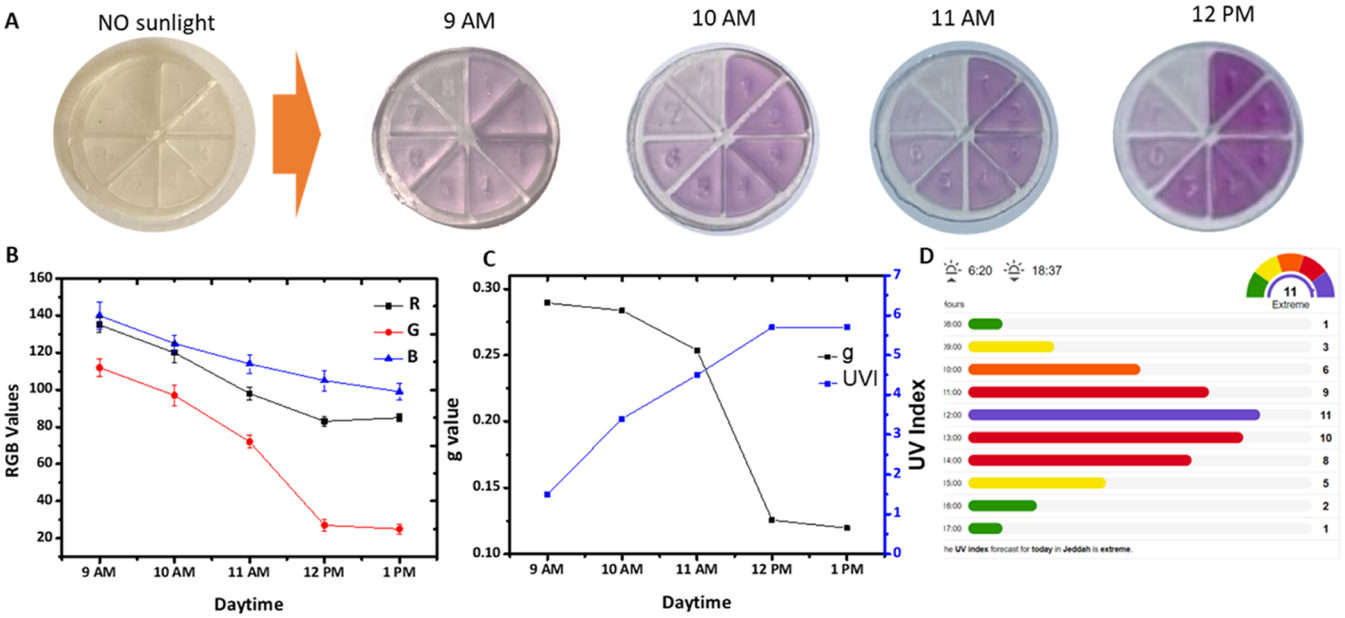

Figure 4. UV detection from RBG values taken from the digital photos of the smart UV watch at different daytimes. (A) The watch is whitish in the shadow, whereas it becomes colorful upon exposure to the sun. Photos are taken every hour from 9 AM to 12 PM. (B) RGB values were recorded from the photos using a mobile application and were presented with respect to the different daytimes. (C) UVI and *g* values are plotted with respect to the different daytimes at each hour. (D) UVI reposted on that day based on a weather forecast web site.

increased when the photographs were measured from darkest to lightest, as shown in Figure 3C.

For UV detection on different daytimes (morning to afternoon), the samples were exposed to sunlight from 9 AM to 12 PM, and photos were captured. The RBG values were obtained from the digital photos of the smart UV watch at different daytimes. The watch is whitish in the shadow, as shown in Figure 4A, whereas it became colorful upon exposure to the sun. The details of the experiment are presented with digital photographs in Figure SI4. The RGB values were recorded and presented with respect to the different days (Figure 4B). The UVI on the same day was obtained from a weather forecast web site and was correlated with the *g* values calculated from the RGB. The UVI and *g* values were plotted with respect to different daytimes (Figure 4C) at each hour.

https://doi.org/10.1021/acsomega.3c07411
ACS Omega 2024, 9, 14830−14839

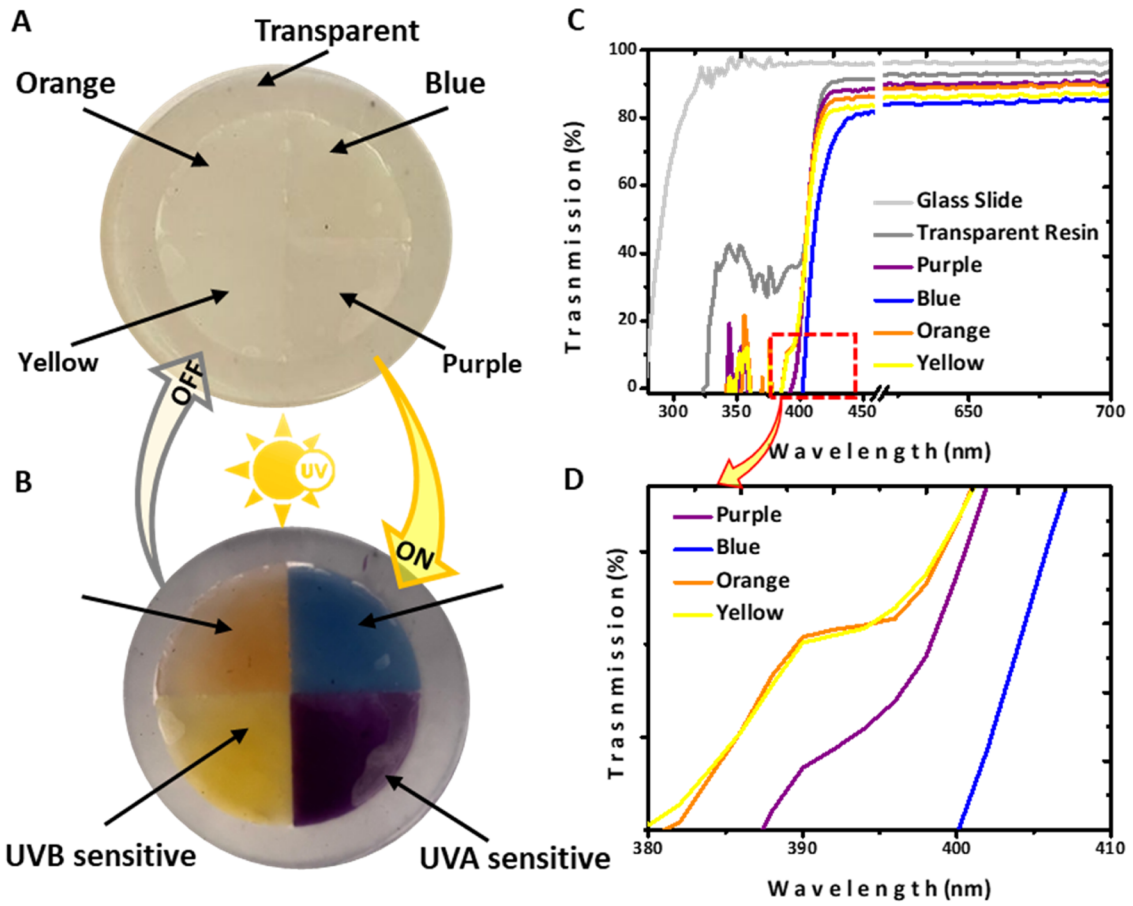

Figure 5. UVA and UVB sensing from the 3D-printed smartwatch. (A) Digital photograph of the smartwatch dial 3D-printed with multiple photochromic pigments in the shadow. (B) The digital photograph of the smartwatch dial 3D-printed with multiple photochromic pigments in sunlight shows the activated photochromic 3D-printed parts. (C) Optical transmission from the different photochromic 3D-printed parts showing the light absorption ranges measured *via* a UV−vis spectrophotometer. (D) The magnified portion of the optical transmission plots presents the UV sensitivity range of different photochromic 3D-printed parts.

The UVI reported on that day based on the weather forecast web site is shown in Figure 4D.

Since commercially available off-the-shelve UV-sensitive materials were utilized in this work while 3D printing the smartwatch, to cross-check the results presented in Figure 4A, the UV index was recorded using a commercial UV meter (Solarmeter Model 6.5 UV Index Meter), and the results are presented in Table S1. The results were further compared with data available from several weather forecast web sites (details are mentioned in the SI). As the intensity of color due to sunlight exposure increases, the recorded UV index increases as well, which confirms the sensitivity of the smart with the change in UV index. The UV index measurement *via* a UV meter and digital photos of the smartwatch (Figure 4) were captured under similar conditions.

By taking advantage of the control over material selection and a multimaterial approach, the smartwatch embedded with four different PC pigments (purple, blue, orange, and yellow) was fabricated *via* DLP 3D printing. The PC pigments are sensitive to different wavelengths of light and absorb UV light in different ranges. This allowed the device to sense a broader range of UV radiation, including UVA and UVB. To identify the wavelength absorbance range of each PC pigment, the samples were printed separately and optical transmission was measured. The results are shown in Figure 5. A digital photograph of the smartwatch embedded with PC pigment, which was captured in the shadow, is shown in Figure 5A. The sensor changed color as soon as it sensed any UV light, as shown in Figure 5B. The light transmission (%T) from 280 to 700 nm was measured, as presented in Figure 5C. The blue PC pigment absorbed all UV wavelengths below 400 nm, indicating that it can be utilized for UVA sensing. Conversely, the purple PC pigment absorbed all UV wavelengths below 380 nm, indicating that it can be applied to sense some of the UVA (Figure 5C). Similarly, orange and yellow PC pigments absorbed UV light below 370 nm, indicating that they could be utilized for UVB along with some portion of UVA (Figure 5D). The development of a multimaterial approach allowed the embedding of multiple materials in the same sensor.

An experiment is being conducted to demonstrate the need for a thickness gradient for sensing UV exposure via colorimetric analysis. The whole without thickness gradient changes its color, whereas the sample with the thickness gradient changes color based on the UV exposure time, as shown in Figure SI5. The smartwatch with 4 compartments, i.e., 4 gradients (Figure SI5A, nongradient, B with gradient) and 8 compartments, i.e., 8 gradients (Figure SI5C, non-gradient, D with gradient), was prepared, and photos were captured in the dark and under sun and presented to realize the effect of gradient. The sample with thickness gradient (the height of the compartment 1−8 kept decreasing) showed nonuniform color change in the presence of UV light as

https://doi.org/10.1021/acsomega.3c07411
ACS Omega 2024, 9, 14830−14839

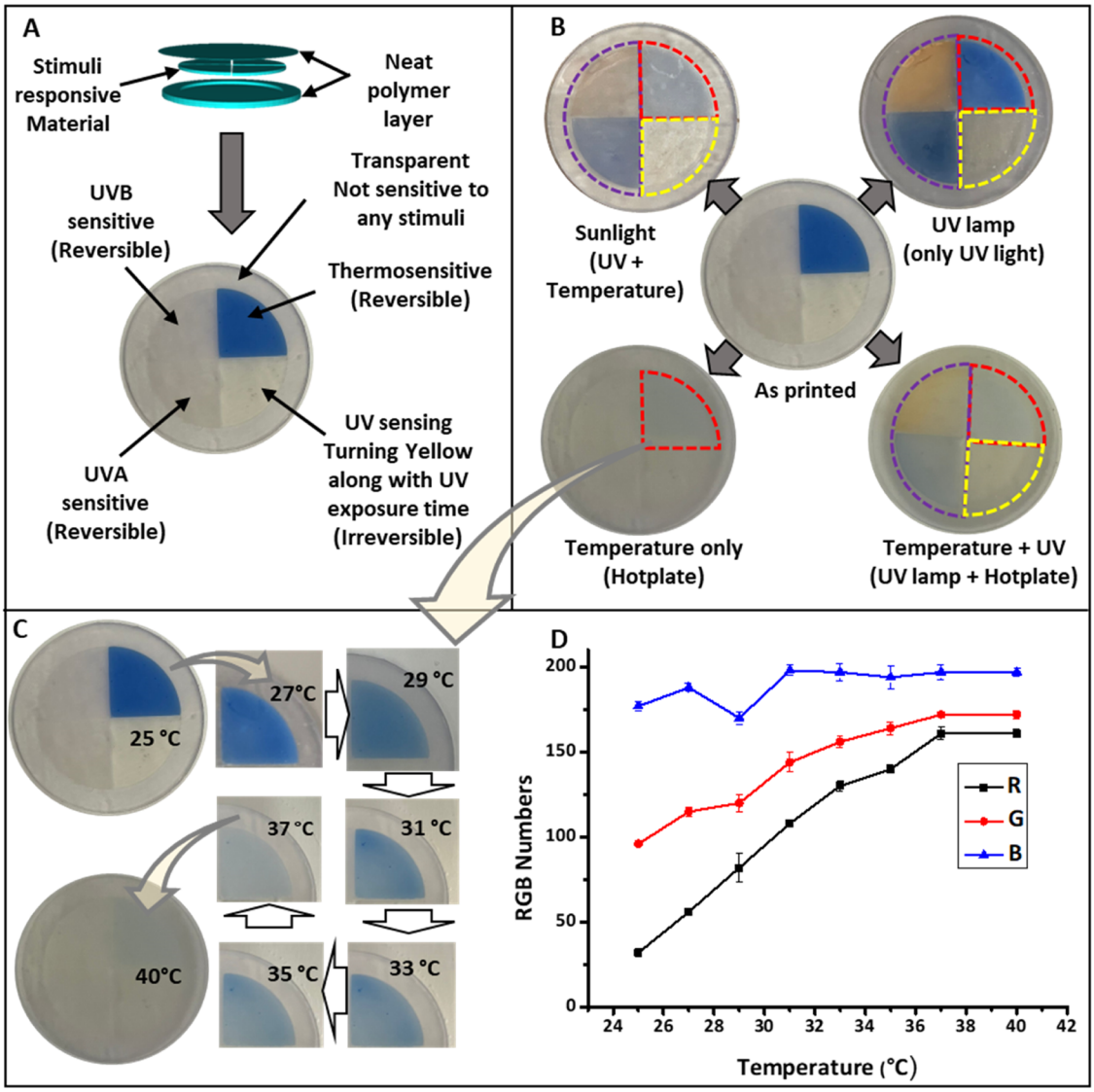

Figure 6. Multifunctional sensor fabricated via a multimaterial approach. (A) CAD model showing the components of the sensor. The multifunctional sensor is printed via multimaterial 3D printing and is shown in the digital photograph, indicating all four embedded sensors. (B) Multiple colorimetric sensing response obtained from the same sensor is presented in the digital photograph. The as-printed sensor is shown in the center, whereas the response to different stimuli is shown by the arrows. (C) Digital photograph showing the change in color in response to a temperature change. (D) The RGB number obtained from the digital photographs taken at a specific temperature of the sensor plotted with respect to the change in temperature.

indicated with the dotted yellow circles, whereas the sample which was nongradient showed uniform color changes in the presence of UV light. The results from this experiment clearly demonstrated the necessity of a thickness gradient for the colorimetric UV sensor.

To develop additional functionality in the 3D-printed smartwatch, the sensor was prepared and embedded with PC pigments of different sensitivities (UVA and UVB), a multifunctional temperature sensor fabricated with PC and TC pigments, and a cumulative UV-sensitive resin that yellows with time, as shown in Figure 6A. The base of the watch was printed with transparent resin, and all four different pre-3D-printed stimuli-sensitive parts were then added. It was followed by printing the top layer of the watch from the transparent resin. The UV and temperature sensing performances of the 3D-printed smartwatch are shown in Figure 6B. When the watch was exposed to sunlight, the PC pigments turned colorful because of the UV rays from the sunlight, whereas the TC pigment started turning colorless. This indicates that the developed sensor can sense UV and temperature changes. In other cases, when the smartwatch was exposed to a UV lamp at room temperature, only the PC gained color and the TC remained unchanged, indicating that the sensor can sense UV light alone. In another case where the smartwatch was exposed to a UV lamp at elevated temperatures, the PC gained color owing to the UV rays, whereas the TC lost color because of the increased temperature. In the fourth case, when the smartwatch was exposed only to elevated temperatures, the PC remained unchanged, whereas the TC lost its color. Using ColorPicker, changes in color in response to UV and temperature, UV exposure, and temperature changes can be monitored. The digital photograph of the temperature sensor changes its color in response to a change in temperature (25 to 40 °C), as shown in Figure 6C. The RGB number obtained

https://doi.org/10.1021/acsomega.3c07411
ACS Omega 2024, 9, 14830−14839

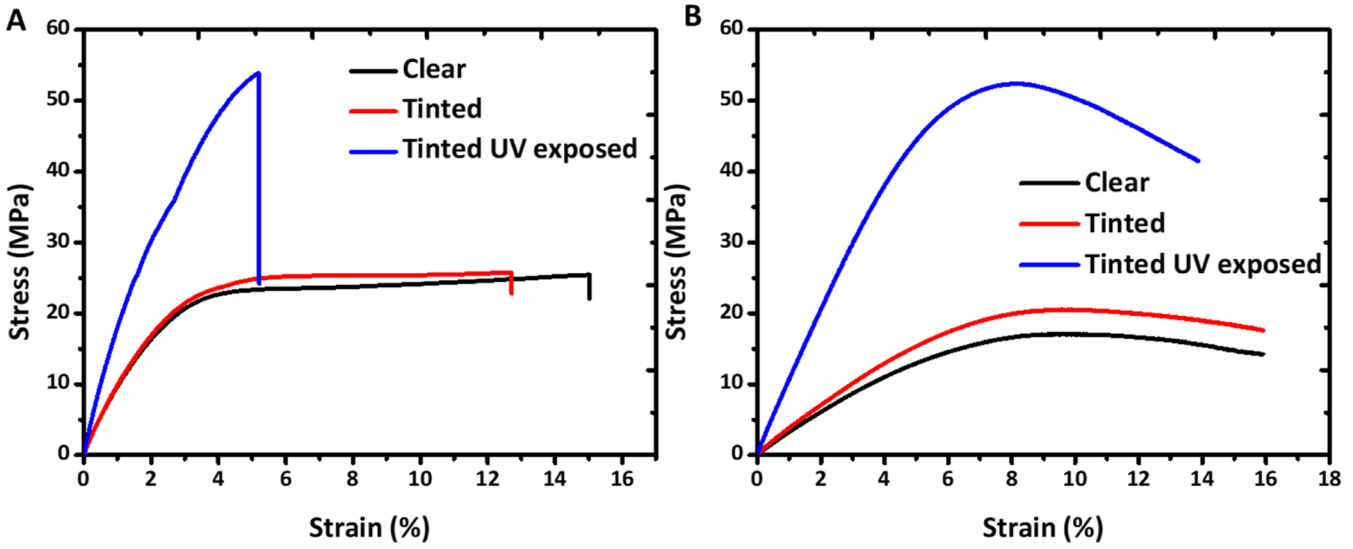

Figure 7. Mechanical property analysis of the 3D-printed specimens. (A) Stress−strain curves obtained from the tensile test. (B) Stress−strain curves obtained from the three-point bending test.

Table 2. Calculated Mechanical Properties from the Tension and 3-Point Bending Tests

test method	properties	clear	tinted	tinted (UV-exposed)
tensile	modulus (MPa)	12.49 ± 0.46	12.07 ± 0.68	21.86 ± 0.74
	strength (MPa)	23.26 ± 1.12	25.05 ± 0.63	54.38 ± 0.82
	elongation (%)	15.01 ± 0.89	12.68 ± 1.03	5.46 ± 0.59
flexural	modulus (MPa)	3.86 ± 0.44	4.86 ± 0.23	12.46 ± 0.77
	strength (MPa)	17.03 ± 1.45	20.53 ± 1.02	52.53 ± 2.45
	deflection (%)	15.95 ± 0.98	15.89 ± 1.17	13.90 ± 0.94

from the digital photographs taken at a specific sensor temperature is plotted with respect to the change in temperature (Figure 6D) which shows that as the pigments become colorless, the RGB values increase. Because the PC and TC pigments are reversible, the sensor regains its original color upon removing the stimuli.

To determine the durability of the 3D-printed smartwatch, tensile and bending properties were measured, and the results are shown in Figure 7. The test specimens were fabricated following the same printing parameters used for the 3D printing of the smartwatch. A sample of clear resin and PC powders were tested and compared. To determine the long-term application response, the specimens were also tested while being exposed to high amounts of UV light. The stress and strain values were calculated from the obtained load−displacement plots, as shown in Figure 7. The stress−strain plots obtained from the tensile tests are presented in Figure 7A, and the resulting plots from the bending tests are shown in Figure 7B. The mechanical properties of the clear resin and tinted samples were significantly similar, indicating that the filler particles did not affect the mechanical properties.

The calculated tensile and flexural mechanical properties, that is, strength modulus and elongation and deflection, are presented in Table 2. It was found that the tensile modulus and strength of the tinted samples were significantly similar, except for a decrease in elongation by approximately 3%.

The prototype of the wearable smartwatch consists of a 3D-printed dial fixed onto a commercially available silicon wristband suitable for all age groups, as shown in Figure 8. Figure 8A shows the printed dial of the smartwatch which can be utilized as a sticker (Figure 8B) or can be fixed into a

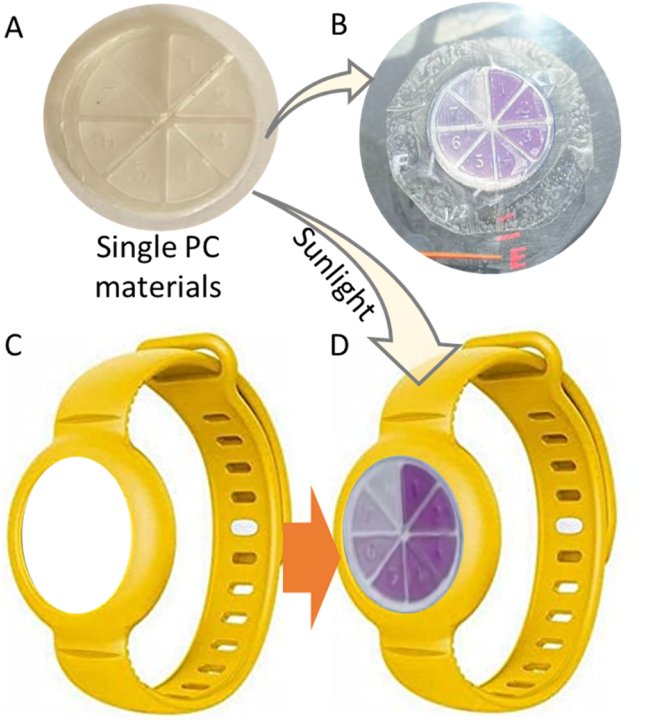

Figure 8. Application of the 3D-printed device as a UV watch and as a sticker. (A) As-printed single watch dial embedded with single photochromic materials, (B) working as sticker, (C) silicon wristband from Amazon, and (d) 3D-printed watch flitted in silicon wristband.

https://doi.org/10.1021/acsomega.3c07411
ACS Omega 2024, 9, 14830−14839

wearable band (Figure 8C). The sticker and the wearable watch are water-resistant and easily removable, making it suitable for multiple outdoor activities such as wearable UV sensor watch, Reading with Mobile Application, UV indication sticker on a child's sun cap, and UV indication sticker on a child's school bag, as shown in Figure SI2. The developed wearable UV sensor will alert users to the extent of UV exposure, helping them protect themselves from overexposure.

4. CONCLUSIONS

The 3D-printed UV-temperature sensor smartwatch was successfully fabricated using a multimaterial 3D printing approach via a vat photopolymerization technique. Photochromic and thermochromic pigments were utilized for UV and temperature sensing using a smartphone application called ColorPicker. PC pigments with different UV sensitivities, UVA (315−400 nm) and UVB (315−280 nm), were utilized to cover a wider range of UV exposure and were mixed in transparent resin. Consequently, the watch was printed with controlled thickness gradients. The 3D-printed UV sensor changes color upon exposure to sunlight. Colorimetric measurements assisted by a smartphone-based application provided the extent of UV exposure from sunlight. The smartwatch can be reused to measure UV exposure because of the reversibility of the sensor when UV light is turned off or brought to the shadow. The mechanical properties of the device were also evaluated to determine its durability in terms of long-term use, and the results showed that the strength of the tinted samples was significantly similar to the clear sample. The wearable watch prototype was prepared by fixing the 3D-printed dial to a commercially available silicon wristband suitable for all age groups. The 3D-printed watch is water-resistant and easily removable, allowing its utilization in multiple outdoor activities. The developed wearable UV sensor alerts the user to the extent of their UV exposure, which can help prevent overexposure.

■ ASSOCIATED CONTENT

Supporting Information

The Supporting Information is available free of charge at https://pubs.acs.org/doi/10.1021/acsomega.3c07411.

Test specimen design for tensile test, potential applications of the UV sensor, and UV index (PDF)

■ AUTHOR INFORMATION

Corresponding Author

Nazek El-Atab − *Electrical Engineering, Computer, Electrical, and Mathematical Sciences and Engineering Division, King Abdullah University of Science and Technology (KAUST), Thuwal 23955-6900, Saudi Arabia;* orcid.org/0000-0002-2296-2003; Email: nazek.elatab@kaust.edu.sa

Authors

Fahad Alam − *Electrical Engineering, Computer, Electrical, and Mathematical Sciences and Engineering Division, King Abdullah University of Science and Technology (KAUST), Thuwal 23955-6900, Saudi Arabia; Materials Science and Engineering Department, King Fahd University of Petroleum and Minerals, Dhahran 31261, Saudi Arabia*

Aljawharah Alsharif − *Electrical Engineering, Computer, Electrical, and Mathematical Sciences and Engineering Division, King Abdullah University of Science and Technology (KAUST), Thuwal 23955-6900, Saudi Arabia*

Fhad O. AlModaf − *Electrical Engineering, Computer, Electrical, and Mathematical Sciences and Engineering Division, King Abdullah University of Science and Technology (KAUST), Thuwal 23955-6900, Saudi Arabia*

Complete contact information is available at: https://pubs.acs.org/10.1021/acsomega.3c07411

Notes

The authors declare no competing financial interest.

■ ACKNOWLEDGMENTS

This study was supported by King Abdullah University of Science and Technology Baseline Fund.

■ REFERENCES

(1) Marković, D.; Petkovska, J.; Mladenovic, N.; Radoičić, M.; Rodriguez-Melendez, D.; Ilic-Tomic, T.; Radetić, M.; Grunlan, J. C.; Jordanov, I. Antimicrobial and UV protective chitosan/lignin multilayer nanocoating with immobilized silver nanoparticles. *J. Appl. Polym. Sci.* **2023**, *140* (19), No. e53823. Liu, Y.; Qin, D.; Wang, H.; Zhu, Y.; Bi, S.; Liu, Y.; Cheng, X.; Chen, X. Effect and mechanism of fish scale extract natural hydrogel on skin protection and cell damage repair after UV irradiation. *Colloids Surf., B* **2023**, *225*, 113281. Suman, G.; Suman, S. Ultraviolet Radiation-Induced Immunomodulation: Skin Ageing and Cancer. In *Skin Aging & Cancer: Ambient UV-R Exposure*; Dwivedi, A.; Agarwal, N.; Ray, L.; Tripathi, A. K., Eds.; Springer: Singapore, 2019; pp 47−58. Buckley, D. Photobiology and the Skin. In *Textbook of Primary Care Dermatology*; Buckley, D.; Pasquali, P., Eds.; Springer International Publishing, 2021; pp 459−466.

(2) McKenzie, R. L.; Lucas, R. M. Reassessing Impacts of Extended Daily Exposure to Low Level Solar UV Radiation. *Sci. Rep.* **2018**, *8* (1), No. 13805. Sánchez-Pérez, J. F.; Vicente-Agullo, D.; Barberá, M.; Castro-Rodríguez, E.; Cánovas, M. Relationship between ultraviolet index (UVI) and first-, second- and third-degree sunburn using the Probit methodology. *Sci. Rep.* **2019**, *9* (1), No. 733. Religi, A.; Backes, C.; Chatelan, A.; Bulliard, J. L.; Vuilleumier, L.; Moccozet, L.; Bochud, M.; Vernez, D. Estimation of exposure durations for vitamin D production and sunburn risk in Switzerland. *J. Exposure Sci. Environ. Epidemiol.* **2019**, *29* (6), 742−752.

(3) Mamahlodi, M. T. Potential benefits and harms of the use of UV radiation in transmission of tuberculosis in South African health facilities. *Journal of public health in Africa* **2019**, *10* (1), 742. From NLM. Ajala, O.; English, P. Dietary Management of Pre-Diabetes and Type 2 Diabetes. In *Glucose Intake and Utilization in Pre-Diabetes and Diabetes*; Watson, R. R.; Dokken, B. B., Eds.; Academic Press, 2015; Chapter 7, pp 85−94.

(4) Lucas, R. M.; Yazar, S.; Young, A. R.; Norval, M.; de Gruijl, F. R.; Takizawa, Y.; Rhodes, L. E.; Sinclair, C. A.; Neale, R. E. Human health in relation to exposure to solar ultraviolet radiation under changing stratospheric ozone and climate. *Photochem. Photobiol. Sci.* **2019**, *18* (3), 641−680. DOI: 10.1039/C8PP90060D.

(5) Dasgupta, A.; Klein, K. Oxidative Stress Induced by Air Pollution and Exposure to Sunlight. In *Antioxidants in Food, Vitamins and Supplements*; Dasgupta, A.; Klein, K., Eds.; Elsevier, 2014; Chapter 3, pp 41−57.

(6) Jin, S. G.; Padron, F.; Pfeifer, G. P. UVA Radiation, DNA Damage, and Melanoma. *ACS omega* **2022**, *7* (37), 32936−32948. From NLM. Zou, W.; González, A.; Jampaiah, D.; Ramanathan, R.; Taha, M.; Walia, S.; Sriram, S.; Bhaskaran, M.; Dominguez-Vera, J. M.; Bansal, V. Skin color-specific and spectrally-selective naked-eye dosimetry of UVA, B and C radiations. *Nat. Commun.* **2018**, *9* (1), No. 3743.

(7) Gao, L.; Liu, Y.; Zhang, M.; Zhao, X.; Duan, Y.; Han, T. Fabricating a photochromic benzonitrile Schiff base into a low-cost

reusable paper-based wearable sensor for naked-eye dosimetry of UV radiations. *Spectrochim. Acta, Part A* **2023**, *295*, No. 122586.
(8) Sharma, M.; Sharma, A. A Review on Nature Based Sunscreen Agents. *IOP Conference Series: Earth Environ. Sci.* **2023**, *1110* (1), No. 012047. Lin, Y.-C.; Chen, Y.-C.; Hwang, B.-F.; Chen, C.-P. Acute dermal effects of solar UV irradiation and efficacy of sunscreen use. *Environ. Pollut. Bioavailability* **2022**, *34* (1), 456−468.
(9) Ghamarpoor, R.; Fallah, A.; Jamshidi, M. Investigating the use of titanium dioxide (TiO2) nanoparticles on the amount of protection against UV irradiation. *Sci. Rep.* **2023**, *13* (1), No. 9793.
(10) Bhattacharjee, S.; Joshi, R.; Chughtai, A. A.; Macintyre, C. R. Graphene Modified Multifunctional Personal Protective Clothing. *Adv. Mater. Interfaces* **2019**, *6* (21), No. 1900622. Baji, A.; Agarwal, K.; Oopath, S. V. Emerging Developments in the Use of Electrospun Fibers and Membranes for Protective Clothing Applications. *Polymers* **2020**, *12* (2), 492.
(11) Backes, C.; Religi, A.; Moccozet, L.; Behar-Cohen, F.; Vuilleumier, L.; Bulliard, J. L.; Vernez, D. Sun exposure to the eyes: predicted UV protection effectiveness of various sunglasses. *J. Exposure Sci. Environ. Epidemiol.* **2019**, *29* (6), 753−764.
(12) Zheng, Y.; Panatdasirisuk, W.; Liu, J.; Tong, A.; Xiang, Y.; Yang, S. Patterned, Wearable UV Indicators from Electrospun Photochromic Fibers and Yarns. *Adv. Mater. Technol.* **2020**, *5* (11), No. 2000564. DOI: https://doi.org/10.1002/admt.202000564 (acccessed 2023/07/13).
(13) Henning, A.; J Downs, N.; Vanos, J. K. Wearable ultraviolet radiation sensors for research and personal use. *Int. J. Biometeorol.* **2022**, *66* (3), 627−640.
(14) Periyasamy, A. P.; Vikova, M.; Vik, M. A review of photochromism in textiles and its measurement. *Text. Prog.* **2017**, *49* (2), 53−136.
(15) Zhao, J.-L.; Li, M.-H.; Cheng, Y.-M.; Zhao, X.-W.; Xu, Y.; Cao, Z.-Y.; You, M.-H.; Lin, M.-J. Photochromic crystalline hybrid materials with switchable properties: Recent advances and potential applications. *Coord. Chem. Rev.* **2023**, *475*, No. 214918.
(16) Pardo, R.; Zayat, M.; Levy, D. Photochromic organic−inorganic hybrid materials. *Chem. Soc. Rev.* **2011**, *40* (2), 672−687. DOI: 10.1039/C0CS00065E.
(17) Kobatake, S.; Terakawa, Y. Acid-induced photochromic system switching of diarylethene derivatives between P- and T-types. *Chem. Commun.* **2007**, No. 17, 1698−1700. DOI: 10.1039/B700177K.
(18) Ma, X.; Wang, X.; Cui, S.; Pu, S. Construction of a Reversible Solid-state Fluorescence Switching Via Photochromic Diarylethene and Si-ZnO Quantum Dots. *J. Fluoresc.* **2024**, *34*, 531.
(19) Lu, H.; Xie, J.; Wang, X.-Y.; Wang, Y.; Li, Z.-J.; Diefenbach, K.; Pan, Q.-J.; Qian, Y.; Wang, J.-Q.; Wang, S.; Lin, J. Visible colorimetric dosimetry of UV and ionizing radiations by a dual-module photochromic nanocluster. *Nat. Commun.* **2021**, *12* (1), No. 2798.
(20) Alam, F.; Elsherif, M.; Salih, A. E.; Butt, H. 3D printed polymer composite optical fiber for sensing applications. *Addit. Manuf.* **2022**, *58*, No. 102996.
(21) Ali, M.; Alam, F.; Ahmed, I.; AlQattan, B.; Yetisen, A. K.; Butt, H. 3D printing of Fresnel lenses with wavelength selective tinted materials. *Addit. Manuf.* **2021**, *47*, No. 102281.
(22) Zhang, Y.; Zhao, X.; Xu, L.; Duan, Y.; Yuan, J.; Li, Z.; Han, T. A turn-on type vapofluorochromic methoxybenzylidene methanone Schiff base applied to wearable VOC sensor and smartphone-based detection. *Sens. Actuators, B* **2024**, *399*, No. 134834.
(23) Wen, G.-Y.; Zhou, X.-L.; Tian, X.-Y.; Hu, T.-Y.; Xie, R.; Ju, X.-J.; Liu, Z.; Pan, D.-W.; Wang, W.; Chu, L.-Y. Real-Time Quantitative Detection of Ultraviolet Radiation Dose Based on Photochromic Hydrogel and Photo-Resistance. *Chem. Mater.* **2022**, *34* (17), 7947−7958.
(24) Jandyal, A.; Chaturvedi, I.; Wazir, I.; Raina, A.; Ul Haq, M. I. 3D printing − A review of processes, materials and applications in industry 4.0. *Sustainable Oper. Comput.* **2022**, *3*, 33−42.
(25) Choi, C.; Okayama, Y.; Morris, P. T.; Robinson, L. L.; Gerst, M.; Speros, J. C.; Hawker, C. J.; Read de Alaniz, J.; Bates, C. M. Digital Light Processing of Dynamic Bottlebrush Materials. *Adv. Funct. Mater.* **2022**, *32* (25), No. 2200883. DOI: https://doi.org/10.1002/adfm.202200883 (acccessed 2023/05/02). Bagheri, A.; Jin, J. Photopolymerization in 3D Printing. *ACS Appli. Polym. Mater.* **2019**, *1* (4), 593−611.
(26) Alam, F.; Ali, M.; Elsherif, M.; Salih, A. E.; El-Atab, N.; Butt, H. 3D printed intraocular lens for managing the color blindness. *Addit. Manuf. Lett.* **2023**, *5*, No. 100129.
(27) Borrello, J.; Nasser, P.; Iatridis, J. C.; Costa, K. D. 3D printing a mechanically-tunable acrylate resin on a commercial DLP-SLA printer. *Addit. Manuf.* **2018**, *23*, 374−380.
(28) Matte, C.-D.; Pearson, M.; Trottier-Cournoyer, F.; Dafoe, A.; Kwok, T. H. Automated storage and active cleaning for multi-material digital-light-processing printer. *Rapid Prototyping J.* **2019**, *25* (5), 864−874. (acccessed 2023/05/02). Shaukat, U.; Rossegger, E.; Schlögl, S. A Review of Multi-Material 3D Printing of Functional Materials via Vat Photopolymerization. *Polymers* **2022**, *14*, No. 2449, DOI: 10.3390/polym14122449.
(29) Vecsei, B.; Czigola, A.; Róth, I.; Hermann, P.; Borbély, J. Digital Impression Systems, CAD/CAM, and STL file. In *Guided Endodontics*; Kinariwala, N.; Samaranayake, L., Eds.; Springer International Publishing, 2021; pp 27−63.
(30) Alam, F.; Shukla, V. R.; Varadarajan, K. M.; Kumar, S. Microarchitected 3D printed polylactic acid (PLA) nanocomposite scaffolds for biomedical applications. *J. Mech. Behav. Biomed. Mater.* **2020**, *103*, No. 103576.
(31) Alam, F.; Elsherif, M.; AlQattan, B.; Salih, A.; Lee, S. M.; Yetisen, A. K.; Park, S.; Butt, H. 3D Printed Contact Lenses. *ACS Biomater. Sci. Eng.* **2021**, *7* (2), 794−803.

https://doi.org/10.1021/acsomega.3c07411
ACS Omega 2024, 9, 14830−14839